Journal of Nuclear Materials 392 (2009) 505–509

Contents lists available at ScienceDirect

Journal of Nuclear Materials

journal homepage: www.elsevier.com/locate/jnucmat

Can redox sensitive radionuclides be immobilized on the surface of spent nuclear fuel? – A model study on the reduction of $Se(IV)_{aq}$ on Pd-doped UO_2 under H_2 atmosphere

Anders Puranen *, Martin Trummer, Mats Jonsson

KTH Chemical Science and Engineering, Nuclear Chemistry, Royal Institute of Technology, SE – 100 44 Stockholm, Sweden

ARTICLE INFO

Article history:
Received 23 December 2008
Accepted 21 April 2009

ABSTRACT

Spent nuclear fuel contains noble metal particles composed of fission products (Pd, Mo, Ru, Tc, Rh and Te, often referred to as ε-particles). Studies have shown that these particles play a major role in catalyzing oxidative dissolution as well as H_2 reduction of the oxidized UO_2 fuel matrix, depending on the conditions. Thus it is possible that these particles also could have a major impact on the state of other redox sensitive radionuclides (such as the long lived fission product ^{79}Se) present in spent nuclear fuel. In this study, Pd-doped UO_2 pellets are used to simulate noble metal particles inclusions in spent nuclear fuel and the effect on dissolved selenium in the form of selenite (250 μM selenite) in simulated ground water solution (10 mM NaCl, 10 mM $NaHCO_3$) at 1 and 10 bar hydrogen pressure. The selenite was found to be reduced to elemental Se, forming colloidal particles. At hydrogen pressures of 10 bar, the rate of selenite reduction was found to be linearly correlated to the fraction of Pd in the UO_2 pellets. No selenium was detected on the surface of the pellets. For the lowest Pd loading (0.1% Pd) the selenite reduction does not appear to proceed to completion indicating that the surface becomes less active.

1. Introduction

Final storage in geological repository is considered by many countries to be the best option for taking care of the highly radioactive waste from the nuclear industry. Although the proposed systems vary in detail among different countries, they always rely on multiple barriers, in order to keep the groundwater from reaching the fuel, and radionuclides from contaminating the biosphere. The safety of such a repository relies on the long term efficiency of the barriers.

Given the very long operational time span for the repository, the safety assessments must be performed on the basis of extreme extrapolations of a number of fairly complicated processes.

One of the key processes here is the dissolution of the spent nuclear fuel matrix in groundwater, liberating radioactive fission products and actinides. The nuclear fuel used in water cooled reactors consists of ceramic uranium dioxide enriched in ^{235}U to 4–5% of the total uranium content. Hence, the spent nuclear fuel consists mainly of UO_2 (>95%), and the rest is fission products and actinides. In granitic groundwaters at the depth of 500–700 m the conditions are reducing and UO_2 has very low solubility [1–3]. However, the ionizing radiation emitted from the fuel will induce chemical processes in the groundwater (radiolysis) producing both oxidants ($OH^{\cdot}$, H_2O_2, $HO_2^{\cdot}$ and O_2) and reductants (e^-_{aq}, $H^{\cdot}$ and H_2) [4]. For kinetic reasons [5], the radiolytically produced oxidants will oxidize U(IV) to the significantly more soluble U(VI) and thereby enhance matrix dissolution.

It has recently been shown that the only oxidant that has to be considered in granitic groundwater is H_2O_2 [6]. The reactions involved in oxidative dissolution are shown in Reactions (1) and (2):

$$UO_{2(s)} + H_2O_2 \rightarrow UO^{2+}_{2(s)} + 2OH^-, \quad (1)$$

$$UO^{2+}_{2(s)} \rightarrow UO^{2+}_{2(aq)}. \quad (2)$$

HCO_3^- present in the groundwater, increases the solubility of U(VI) and thereby the rate of fuel matrix dissolution even further [7–11]. This results in the release of radionuclides contained by the matrix. In this study, 10 mM HCO_3^- and 10 mM NaCl was used to simulate groundwater and to keep any U(VI) species from precipitating. The solution also buffers the pH at ~8 and provides a nearly constant ionic strength so as to keep these factors close to constant during the experiments.

In Sweden, and some other countries planning geological repositories for spent nuclear fuel, one of the barriers in the system is a copper canister with an iron insert. In case of system failure, the canister will be exposed to anoxic groundwater. Iron will undergo anaerobic corrosion producing magnetite and hydrogen (Reaction (3)) [12]:

$$3Fe + 4H_2O \rightarrow Fe_3O_4 + 4H_2. \quad (3)$$

* Corresponding author.
E-mail address: puranen@kth.se (A. Puranen).

0022-3115/$ - see front matter © 2009 Elsevier B.V. All rights reserved.
doi:10.1016/j.jnucmat.2009.04.019

Hydrogen is also produced by radiolysis of water, but the amount produced from iron corrosion is significantly larger. H_2 has been shown to have a considerable inhibiting effect on the dissolution of spent nuclear fuel [13–16], and thereby the release of radionuclides. Two major pathways for inhibition of oxidative dissolution of spent nuclear fuel have been identified: (1) competitive consumption of oxidants and (2) reduction of oxidized UO_2 on the surface. These processes can be seen in Reactions (4) and (5):

$$Ox + H_2 \rightarrow Red + 2H^+, \quad (4)$$

$$UO^{2+}_{2(s)} + H_2 \rightarrow UO_{2(s)} + 2H^+. \quad (5)$$

Both processes (Eqs. (4) and (5)) depend on catalytic noble metal particles composed of fission products (Pd, Mo, Ru, Tc, Rh and Te, often referred to as ε-particles) [17,18]. Reaction (5) fully accounts for the observed decrease in UO_2 matrix dissolution and release of radionuclides in spent nuclear fuel leaching experiments under H_2 atmosphere [19].

One of the concerns in the safety assessment for geological repositories is the fission product ^{79}Se. Although the amount of ^{79}Se in the spent fuel matrix is relatively low (depending on burn up, fission yield of approximately 0.04%) at the time of discharge, its long half-life (reported in the range of 10^5–10^6 y [20,21]) and the potentially high mobility of dissolved Se-anions explain the importance. Selenium may exist as selenate, Se(VI) and selenite, Se(IV) in solution, or as the more sparingly soluble selenides Se(-II), Se(-I) and zero valent Se(0).

A multitude of studies have been performed on the fate of dissolved selenium under reducing conditions, particularly with respect to its interaction with iron oxides and hydroxides [22–28] or microbial reduction [29], including effects of gaseous hydrogen on the microbial reduction [30].

However, there is no published data on the possible immobilization of dissolved Se due to noble metal catalyzed reduction by H_2 (summarized for Se(IV) in Eq. (6)):

$$Se(IV) + 2H_2 \xrightarrow{Pd} Se(0) + 4H^+. \quad (6)$$

In the present paper, we study the reduction of selenite (kinetics and speciation) by UO_2 pellets, doped with 0.1%, 1% and 3% Pd-particles in solution under H_2 atmosphere.

2. Experimental

The palladium doped uranium dioxide pellets used in this study were hot pressed under vacuum from depleted UO_2 (Westinghouse Atom AB) and palladium powder (Aldrich, 99,9+% Pd, a,v particle size 1–2 μm) yielding pellets of 13 mm diameter and 2.6 mm thickness with a surface area of ~372 mm^2. Details on the production of the pellets are given in [18].

Prior to the experiments the pellets were cleaned by ultrasonication for 30 s in a 20 mM $NaHCO_3$ solution, transferred to a glove box (nitrogen, <5 ppm O_2) and stored overnight in a fresh 20 mM $NaHCO_3$ solution. The pellets were placed in glass vessels with 5 ml of 10 mM NaCl, 10 mM $NaHCO_3$ and 250 μM Na_2SeO_3 (pH ~8.2). All solutions were prepared inside the glove box from degassed Milli-Q deionized water (18 MΩ). The glass vessels were sealed in an autoclave, transferred out of the glove box, purged with hydrogen (Air Liquid, Hydrogen+) and pressurized with H_2 to either 1 or 10 bar absolute at room temperature. For sampling, the autoclave was transferred back into the glove box, and the Se(IV) concentration in the samples was measured by iodometry at 350 nm (under oxygen free conditions), using a Jasco V-630 UV/VIV spectrophotometer. All samples were centrifuged (RCF 25 000g) prior to analysis.

The composition and morphology of the surfaces were investigated using SEM–EDS, Scanning Electron Microscope–Energy Dispersive X-ray spectroscopy (JEOL JSM 9460LV). In addition, a Raman spectrometer (Renishaw 1000 system) with a 633 nm Spectra Physics model 127 laser was used. The Raman spectra were recorded at room temperature using 20× and 80× magnification, corresponding to a spatial resolution of 5 μm or less. Colloidal solutions were investigated by PCS, Photon Correlation Spectroscopy using a 488 nm dynamic light scattering instrument 90 Plus Particle Size Analyser with a 2 W Lexus Laser Model 95 Ion Laser. Samples of the dried in colloids were also investigated by TEM, Transmission Electron Microscopy (Philips Tecnai 10).

3. Results

3.1. Reaction dynamics

The pH in the experiments (buffered by the presence of 10 mM $NaHCO_3$) remained stable at ~8 during the course of all experiments. The composition and labeling of the samples is described in Table 1. As can be seen in Fig. 1(a) for sample 3–10, the rate of selenite removal was considerably higher than for sample 1–10, followed by sample 0.1–10 which displayed the slowest reaction dynamics. Sample 0.1–10 reaches a plateau after removal of ~40% of the selenite, possibly due to blockage of the surface or poisoning of the Pd catalyst. Poisoning of Pd catalysts is documented for reduced sulfur species [31] which could be suspected to behave in an analogous way to reduced Se species. Data on Se poisoning of Pd catalysts is however scarce, although it has been observed for organic Pd catalysts [32].

Using the rates of reduction for the experiments and the estimated surface area of the pellets, the overall rate constant for the pellet (in $m\,s^{-1}$) can be determined. By plotting the overall rate constant against the Pd fraction, the second order rate constant for the Pd-catalyzed reduction can be determined. As can be seen in Fig. 2, there is a linear correlation between the rate constant (expressed as a second order rate constant on the basis of the total surface area) and the Pd fraction under these conditions, corresponding to a second order rate constant of $2.5 \pm 0.3 \times 10^{-7}$ $m\,s^{-1}$ with respect to the Pd surface area for the experiments at 10 bar. Comparison of the rate constant at 10 bar H_2 with the previously determined one [33] for the reaction with the same pellets and hydrogen peroxide (at equivalent hydrogen pressure) gives a difference by nearly two orders of magnitude lower for this work. The reduction of selenite is, thus, significantly slower than that of hydrogen peroxide under these conditions. This is also expected given the difference in thermodynamic driving force for the two reaction systems. The standard potential of selenite, assuming a path according to Reaction (7), at pH 8 was calculated to ~0.19 V vs. SHE using data from, Ref. [34]. The reduction potential of hydrogen peroxide (according to Reaction (8)) at the same pH was calculated to ~1.3 V vs. SHE

Table 1
Composition of the samples. All samples contain 10 mM NaCl, 10 mM $NaHCO_3$ and 250 μM Na_2SeO_3. The labeling refers to the Pd-content and H_2 pressure of each sample.

Samples	Pd fraction	H_2 pressure (bar)
0.1–10	0.1	10
1–1	1	1
1–10	1	10
3–1	3	1
3–10	3	10

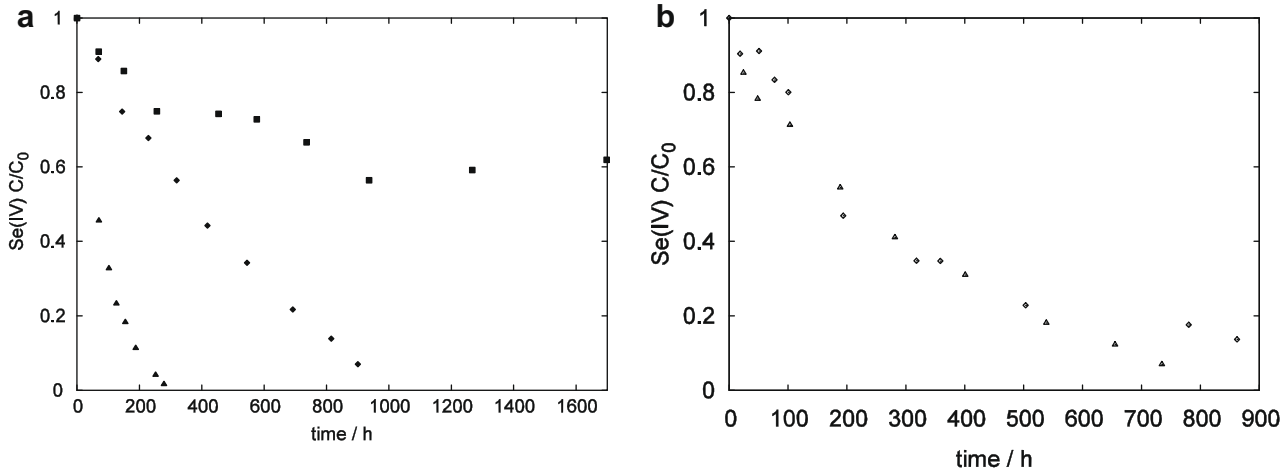

Fig. 1. Normalized Se(IV) concentrations vs. time. (a) 10 bar H_2: ▲, 3% Pd; ♦, 1% Pd; ■, 0.1% Pd. (b) 1 bar H_2: Δ, 3% Pd; ◇, 1% Pd. The anaytical error is estimated to ~10%.

$$HSeO_3^- + 5H^+ + 4e^- \rightarrow Se + 3H_2O, \quad (7)$$

$$H_2O_2 + 2H^+ + 2e^- \rightarrow 2H_2O. \quad (8)$$

The experiments performed (Fig. 1(b)) at 1 bar H_2 resulted in approximately the same rate for the 1% Pd-pellet but with a considerably slower reduction of Se(IV) for the 3% Pd-pellet compared to the experiments at 10 bar H_2. The overall second order rate constants (with respect to the pellet surface area) for the different cases are given in Table 2.

The selenite concentration remained constant for >2000 hours in a parallel experiment using a UO_2 powder suspension under 25 bar H_2 pressure (same solution composition as in the pellet experiments) where the solid surface area to solution volume ratio was higher than in the pellet experiments. This indicates that Pd is the critical component for Se(IV) reduction to occur and that Se(IV) adsorption on UO_2 is very limited under the present conditions.

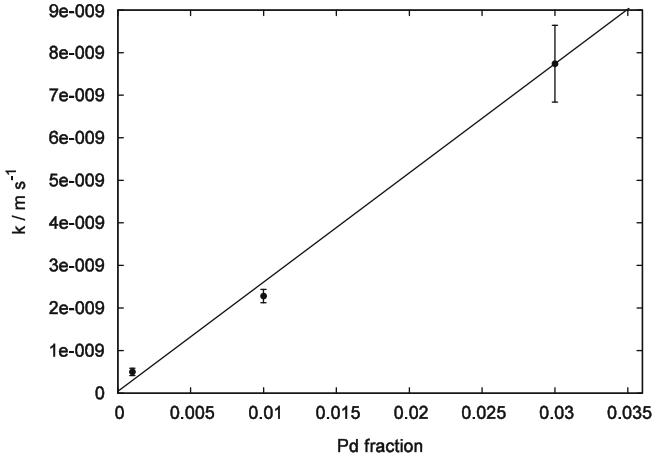

Fig. 2. Second order rate constants for the selenite reduction vs. Pd fraction under 10 bar H_2.

Table 2
Overall second order rate constants for the reduction of selenite based on the total pellet surface area ($m\ s^{-1}$).

	0.1% Pd	1% Pd	3% Pd
1 bar H_2	–	$(2.2 \pm 0.8) \times 10^{-9}$	$(3.2 \pm 0.9) \times 10^{-9}$
10 bar H_2	$(5.0 \pm 0.9) \times 10^{-10}$	$(2.3 \pm 0.2) \times 10^{-9}$	$(7.7 \pm 0.9) \times 10^{-9}$

3.2. Product characterization

When less than 5% of the initial selenite concentration remained in sample 3–10 the previously transparent solution turned faint orange/red with a small amount of red particles on the bottom of the vessel, indicating that colloids had formed.

PCS, Photon Correlation Spectroscopy was used to verify the existence of colloids in the solutions from the 10 bar H_2 experiments after ~1500 h reaction time. The sample solutions were transferred out of the glove box and measured immediately. Significant amounts of colloids were detected in samples 1–10 and 3–10. However, due to the lack of reference material the amount of colloidal material could not be quantified. As can be seen in Fig. 3, the hydrodynamic diameter was around 150 nm for samples 1–10 and 3–10. The colloid concentration in sample 0.1–10 was too low as to allow a qualitative size distribution. It must be noted that the relative intensity scale in Fig. 3 only relates to the size distribution of the individual sample and that it cannot be used to compare amounts of colloidal particles between samples. Centrifugation (RCF 25 000*g*) of the solutions removes all detectable colloids giving bright red precipitates.

The colloids were also studied by TEM. Solutions from the experiments were diluted by distilled water and a few drops were applied to and left to dry on cupper TEM grids (in the dry anoxic atmosphere of the glove box). The use of ethanol was avoided in

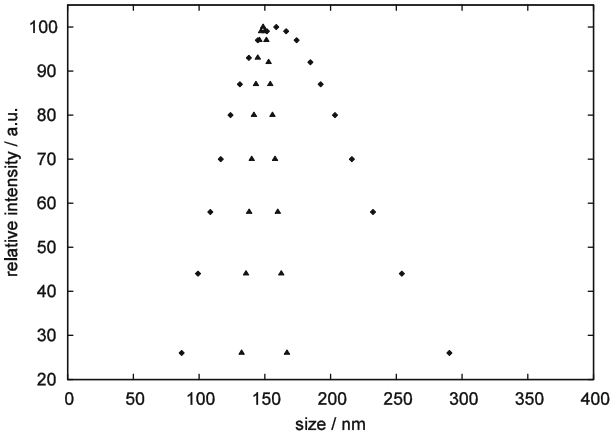

Fig. 3. PCS size distribution of 10 bar H_2 samples at ~1500 h. ▲: 3%-Pd; 1.4 Mcps. ♦: 1%-Pd, 627 kcps. Background count rate: ~30 kcps.

the TEM preparation due to potential ethanol induced Se allotrope transformations [35]. Particles of ~50–100 nm diameter were present in the TEM samples, as can be seen in Fig. 4 showing a picture from sample 0.1–10. No particles were observed in a blank TEM-grid prepared together with the TEM-samples exposed only to the distilled water used in the experiments. Selected area electron diffraction of the particles did not yield any distinctive patterns, indicating that the particles are likely amorphous. Powder X-ray diffraction of the red precipitate from experiments (dried in the glove box) also lacked any distinctive reflexes, supporting the case that the product is amorphous.

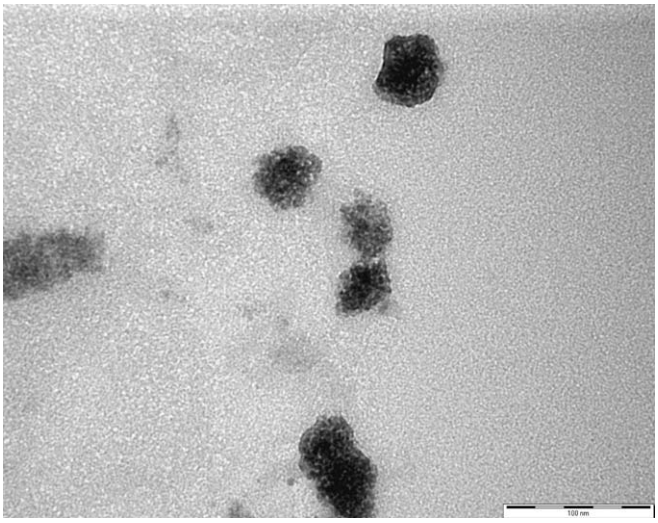

Fig. 4. TEM image of colloids from sample 0.1–10.

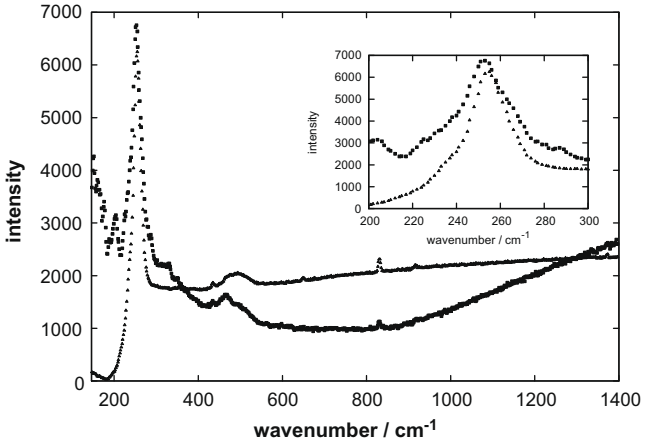

Fig. 5. Raman spectra of red particles from sample 3–10 and elemental Se reference.

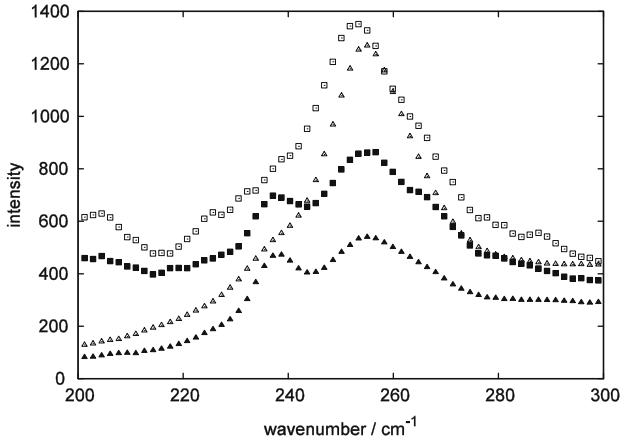

Fig. 6. Raman spectra of the effect of prolonged illumination on sample 3–10 and the Se reference. □: Se reference; Δ: sample 3–10; ■: Se reference after prolonged illumination; ▲: sample 3–10 after prolonged illumination.

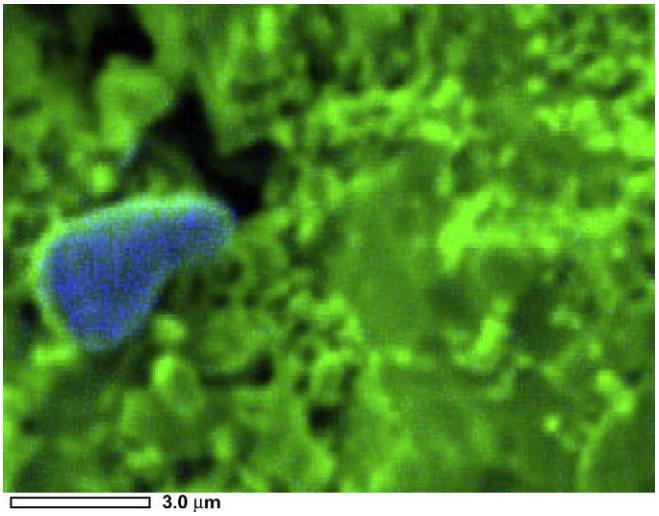

Fig. 7. Bicolor SEM–EDS map of sample 3–10. Uranium (green); palladium (blue). (For interpretation of the references to colour in this figure legend, the reader is referred to the web version of this article.)

Samples of the dried in colloidal solutions and precipitates were also investigated by Raman spectroscopy. The main feature of the spectra of the red solids is a strong band at ~255 cm^{-1} (Fig. 5). Measurements on a predominantly monoclinic elemental selenium standard (confirmed by XRD measurement) displayed a band at ~253 cm^{-1}. A difference of 2 cm^{-1} is assumed to be within the limits of the spectral resolution of the instrument. The differentiation between Raman bands from amorphous and monoclinic elemental Se allotropes is however difficult since amorphous Se is also assigned positions at ~250–255 cm^{-1} [36,37].

Further evidence of elemental selenium in the investigated samples is the partial photoinduced transformation of the assigned elemental Se bands at ~253–255 cm^{-1} to trigonal elemental selenium (band at ~237 cm^{-1}) [36] that occurs in the samples as well as for the Se reference material after prolonged laser illumination (Fig. 6).

The pellet from sample 3–10 was removed from its solution and allowed to dry inside the glove box and fixated on a SEM-template with copper tape. SEM–EDS mapping of the pellet surfaces (Fig. 7) revealed Pd-grains in the uranium dioxide matrix. No selenium was detected on the surface of the pellet indicating very limited attachment of selenium to the surfaces, or that a selenium layer is of such a limited thickness that it is undetectable by SEM–EDS.

4. Conclusions

Selenite was found to be reduced to elemental Se by H_2 in the presence of Pd-doped UO_2. The elemental Se was at least partly in the form of colloidal particles with an approximate size of 100 ± 50 nm (PCS and TEM). Based on the Raman spectra supported by the absence of diffraction patterns (TEM–SAED and XRD) we conclude that the Se is predominantly amorphous. No Se was detected on the surface of the pellets (by SEM–EDS) indicat-

ing that adsorption of the elemental Se product was limited. However, for the lowest Pd loading (0.1% Pd) the selenite reduction does not appear to proceed to completion indicating that the surface becomes less active. This apparent self-inhibition coupled with the uncertainties such as the actual pellet surface area and the accessible Pd surface area makes accurate determination of the kinetic parameters precarious. For 10 bar hydrogen pressure, the rate of selenite reduction was nevertheless found to be linearly correlated to the fraction of Pd in the UO_2 pellets with a second order rate constant of $2.5 \pm 0.3 \times 10^{-7}$ m s^{-1} with respect to Pd on the surface. Despite the unfavorable surface area to solution volume ratio, a large amount of selenite was reduced by H_2 in the presence of Pd-doped UO_2. This illustrates that dissolved redox sensitive radionuclides, such as selenite, can be reduced by H_2 on noble metal particles in spent nuclear fuel. Although the stability and further fate of the formed Se colloids is outside the scope of this paper, it illustrates that reduction of dissolved species into sparingly soluble forms is not necessarily a process that is synonymous with immobilization of the species.

Acknowledgement

The Swedish Nuclear Fuel and Waste Management Co (SKB) is gratefully acknowledged for financial support.

References

[1] R.L. Segall, R.S.C. Smart, J. Nowotny, Surface and Near-Surface Chemistry of Oxide Materials, Elsevier Science Publishers B.V., Amsterdam, Netherlands, 1988. p. 527.
[2] D. Rai, A.R. Felmy, J.L. Ryan, Inorg. Chem. 29 (1990) 260.
[3] I. Casas, J. de Pablo, J. Giménez, M.E. Torrero, J. Bruno, E. Cera, R.J. Finch, R.C. Ewing, Geochim. Cosmochim. Acta 62 (1998) 2223.
[4] J.W.T. Spinks, R.J. Woods, An Introduction to Radiation Chemistry, John Wiley, New York, 1964. p. 477.
[5] O. Roth, M. Jonsson, Cent. Eur. J. Chem. 6 (2008) 1.
[6] E. Ekeroth, O. Roth, M. Jonsson, J. Nucl. Mater. 355 (2006) 38.
[7] I. Grenthe, F. Diego, F. Salvatore, G. Riccio, J. Chem. Soc. Dalton Trans. 11 (1984) 2439.
[8] J. de Pablo, I. Casas, J. Giménez, M. Molera, M. Rovira, L. Duro, J. Bruno, Geochim. Cosmochim. Acta 63 (1999) 3097.
[9] D.E. Grandstaff, Econ. Geol. 71 (1976) 1493.
[10] W.J. Gray, J.C. Tait, S.A. Steward, D.W. Shoesmith, High Level Radioactive Waste Management, V Annual International Conference, La Grange Park, IL, 1994. p. 2597.
[11] E.M. Pierce, J.P. Icenhower, R.J. Serne, J.G. Catalano, J. Nucl. Mater. 345 (2005) 206.
[12] N.R. Smart, D.J. Blackwood, L. Werme, SKB Tech. Rep. TR-01-22 (2001).
[13] P. Carbol, J. Cobos-Sabathe, J.-P. Glatz, C. Ronchi, V. Rondinella, D.H. Wegen, T. Valiente, SKB Tech. Rep. TR-05-09 (2005).
[14] T.E. Eriksen, M. Jonsson, SKB Tech. Rep. TR-07-06, August 2007.
[15] K. Spahiu, J. Devoy, D. Cui, M. Lundström, Radiochim. Acta 92 (2004) 597.
[16] S. Rollin, K. Spahiu, U.-B. Eklund, J. Nucl. Mater. 297 (2001) 231.
[17] S. Nilsson, M. Jonsson, J. Nucl. Mater. 372 (2008) 160.
[18] M. Trummer, S. Nilsson, M. Jonsson, J. Nucl. Mater. 378 (2008) 55.
[19] M. Jonsson, F. Nielsen, O. Roth, E. Ekeroth, S. Nilsson, M.M. Hossain, Environ. Sci. Technol. 41 (2007) 7087.
[20] C.-M. Zhou, Z.-D. Wu, Nucl. Sci. Tech. 17 (1) (2006) 21.
[21] M. He, S. Jiang, S. Jiang, L. Diao, S. Wu, C. Li, Nucl. Instrum. and Meth. B B194 (2002) 393.
[22] A.P. Murphy, Indust. Eng. Chem. Res. 27 (1988) 187.
[23] Y. Zhang, J. Wang, C. Amrhein, W.T. Frankenberger Jr., J. Environ. Qual. 34 (2005) 487.
[24] S.C.B. Myneni, T.K. Tokunaga, G.E. Brown, Science 278 (1997) 1106.
[25] S.R. Qiu, H.F. Lai, M.J. Roberson, M.L. Hunt, C. Amrhein, L.C. Giancarlo, G.W. Flynn, J.A. Yarmoff, Langmuir 16 (2000) 2230.
[26] A.M. Scheidegger, D. Grolimund, D. Cui, J. Devoy, K. Spahiu, P. Wersin, I. Bonhoure, M. Janousch, J. Phys. IV: Proc. 104 (2003) 417.
[27] R. López de Arroyabe Loyo, S.I. Nikitenko, A.C. Scheinost, M. Simonoff, Environ. Sci. Technol. 42 (2008) 2451.
[28] A.C. Scheinost, L. Charlet, Environ. Sci. Technol. 42 (2008) 1984.
[29] J.F. Stolz, P. Basu, R.S. Oremland, Int. Microbiol. 5 (2002) 201.
[30] R.S. Oremland, J.T. Hollibaugh, A.S. Maest, T.S. Presser, L. Miller, C. Culbertson, Appl. Environ. Microbiol. 55 (1989) 2333.
[31] N. Munakata, M. Reinhard, Appl. Catal. B: Environ. 75 (2007) 1.
[32] S.I. Fukuzawa, T. Fujinami, S. Sakai, Chem. Lett. 19 (1990) 927.
[33] M. Trummer, O. Roth, M. Jonsson, J. Nucl. Mater. 383 (2008) 226.
[34] F. Séby, M. Potin-Gautier, E. Giffaut, G. Borge, O.F.X. Donard, Chem. Geol. 171 (2001) 173.
[35] S.Y. Xie, C.F. Wang, X.H. Zhang, Z.Y. Jiang, Z.X. Xie, Z.Q. Tian, R.B. Huang, L.S. Zheng, J. Mater. Chem. 13 (2003) 1447.
[36] V.V. Poborchii, A.V. Kolobov, K. Tanaka, Appl. Phys. Lett. 72 (1998) 1167.
[37] S.N. Yannopoulos, K.S. Andrikospoulos, J. Chem. Phys. 121 (2004) 4747.